

AperTO - Archivio Istituzionale Open Access dell'Università di Torino

Geology of the Fontane talc mineralization (Germanasca valley, Italian Western Alps)

This is the author's manuscript

Original Citation:

Availability:

This version is available <http://hdl.handle.net/2318/1566203> since 2018-07-16T16:07:13Z

Published version:

DOI:10.1080/17445647.2016.1142480

Terms of use:

Open Access

Anyone can freely access the full text of works made available as "Open Access". Works made available under a Creative Commons license can be used according to the terms and conditions of said license. Use of all other works requires consent of the right holder (author or publisher) if not exempted from copyright protection by the applicable law.

(Article begins on next page)



UNIVERSITÀ DEGLI STUDI DI TORINO

1
2
3
4
5
6
7
8
9
10

This is an author version of the contribution published on:

Questa è la versione dell'autore dell'opera:

[Journal of Maps, 10.1080/17445647.2016.1142480]

ovvero [Paola Cadoppi, Giovanni Camanni, Gianni Balestro, Gianluigi

Perrone, Taylor & Francis, 2016]

The definitive version is available at:

La versione definitiva è disponibile alla URL:

[<http://dx.doi.org/10.1080/17445647.2016.1142480>]

11 **Geological map of the Fontane Talc Mineralization (Germanasca**
12 **Valley, Italian Western Alps)**

13

14 Paola Cadoppi¹, Giovanni Camanni², Gianni Balestro^{1*} and Gianluigi Perrone¹

15

16

17

18 ¹ Department of Earth Sciences, University of Torino, Via Valperga Caluso, 35, 10125
19 Torino, Italy

20

21 ² Fault Analysis Group, School of Geological Sciences, University College Dublin,
22 Belfield Dublin 4, Ireland

23

24

25 ***Corresponding Author:**

26 Gianni Balestro

27 email: gianni.balestro@unito.it

28

29

30 **Submitted to:**

31 Journal of Maps

32

33

34

35

36

37

38

39

40

41 **Abstract**

42 The 1:5,000 scale Geological Map of the Fontane Talc Mineralization aims to give new
43 information about the origin and geological structure of an important talc mineralization
44 occurring in the axial sector of the Italian Western Alps. The Fontane Talc
45 Mineralization is hosted within a pre-Carboniferous polymetamorphic complex which
46 was deformed and metamorphosed during both Variscan and Alpine orogenesis, and is
47 part of the Dora-Maira continental crust. Field mapping and underground investigations
48 highlight that the talc bodies (*i*) never crop out but occur at depth along a well-defined
49 lithostratigraphic association between micaschist, marble and gneiss, and (*ii*) were
50 deformed during different Alpine-related deformation phases (i.e. D₁, D₂ and D₃ syn-
51 metamorphic phases and post-metamorphic extensional faulting). The here defined
52 lithostratigraphic and structural characterization of talc bodies, is a input for further
53 researches onto geodynamic context wherein talc formed and for new mineral
54 exploration outside the mapped area.

55

56

57

58

59

60 Keywords: Western Alps; Talc mineralization; Alpine tectonics; extensional faulting

61

62

63 **1. Introduction**

64 One of the industry-related geological features of the Italian Western Alps is a
65 discontinuous, several kilometre-wide belt of talc mineralizations (throughout the paper
66 we define talc mineralization a geological body with a significant content in talc). The
67 most important of these mineralizations (and one of the most important in Europe), due
68 to both quantity and quality of the extracted talc, is located in the Germanasca Valley
69 (Italian Western Alps) and is known as the Fontane Talc Mineralization (FTM
70 hereafter) (Grill et al., 1955; Peretti, 1966; Zucchetti, 1969, 1972; Sandrone et al., 1987,
71 1990; Sandrone & Zucchetti, 1989). The FTM is hosted within a pre-Carboniferous
72 polymetamorphic complex which was deformed and metamorphosed during both
73 Variscan and Alpine orogenesis, and is part of the Dora-Maira continental crust
74 (Sandrone et al., 1993) (Fig. 1).

75 Despite its industrial significance, both origin and geological structure of the FTM has
76 been never defined in detail, and published map exists only at small scale (i.e., the
77 Pinerolo sheet of the Geological Map of Italy at 1:100,000 scale; Mattiolo et al., 1913).
78 In this paper, we present a new 1:5,000 scale geological map that spans an area of about
79 8 km² above the main infrastructures (i.e., tunnels) of both past and current extraction
80 sites, with the aim of further advancing knowledge about geology of the FTM. Since the
81 talc bodies never crop out, we have integrated the map with geological cross sections
82 that allow identifying their location at depth, as well as defining their geometry and
83 lithostratigraphic association with embedding rocks.

84

85 **2. Methods**

86 The geological map presented in this study is the result of fieldwork carried out at
87 1:5,000 scale. Lithological observations and collection of structural data were
88 performed both in the field and in underground locations. Data were stored in a GIS
89 database (Coordinate System WGS 1984 UTM Zone 32N) and represented on a raster
90 topographic map derived from “Carta Tecnica Provinciale” 1:5,000 (“Dai tipi di
91 proprietà della Città Metropolitana di Torino - Servizio Cartografico”,
92 authorization n.105625/2015 on July 21, 2015).

93 The geological map includes (*i*) three cross sections localized in the area where talc is
94 currently being extracted and defined through an integration of field data with borehole
95 data (i.e., data available from companies holding the mining concession over the years),

96 and (ii) a 1:20,000 scale tectonic map wherein geological interpolation, interpretation
97 and generalization of outcrops and structures are given.

98

99 **3. Regional setting**

100 The FTM is located along the western edge of the Dora-Maira, a slab of paleo-European
101 continental crust which belongs to the Penninic Domain of the Western Alps (Fig. 1)
102 (see e.g. Bigi et al., 1990; Dal Piaz et al., 2003). The Dora-Maira (Vialon, 1966;
103 Sandrone et al., 1993; Cadoppi et al., 2002) was involved in Alpine-related E-dipping
104 subduction, W-verging continental collision and deep crust/mantle indentation (see e.g.
105 Wheeler, 1991; Chopin et al., 1991), and is now stacked in the axial sector of the
106 Western Alps and tectonically overlain by blueschist-facies and eclogite-facies meta-
107 ophiolite units (i.e., the Queyras Schistes Lustrès Complex and the Monviso Meta-
108 ophiolite Complex, respectively; see e.g., Tricart and Schwartz, 2006; Balestro et al.,
109 2014).

110 In its northern sector, the Dora-Maira comprises two main superposed units that, during
111 Alpine orogeny, were metamorphosed under different P–T peak conditions (Fig. 1). The
112 upper one corresponds to an eclogite-facies polymetamorphic complex, which consists
113 of metasediments and Upper Ordovician meta-intrusives (Bussy and Cadoppi, 1996)
114 covered by thin Mesozoic carbonate metasediments; the lower one consists of a
115 blueschist-facies Permo-Carboniferous monometamorphic complex (i.e., the Pinerolo
116 Graphitic Complex; Vialon, 1966; Borghi et al., 1984; Sandrone et al., 1993). Both
117 complexes contain meta-intrusives of granitic to dioritic composition, which can be
118 related to a late Variscan magmatic event (Bussy & Cadoppi, 1996).

119 The FTM is included within the upper, polymetamorphic complex, which was affected
120 by Variscan-related medium-grade metamorphism, and, after the Alpine-related
121 eclogite-facies metamorphism, was pervasively re-equilibrated under blueschist- and
122 greenschist-facies metamorphic conditions (Sandrone et al., 1987, 1990; Borghi and
123 Sandrone, 1990; Cadoppi, 1990; Cadoppi and Tallone, 1992; Damiano, 1997; Camanni,
124 2010).

125

126 **4. Lithostratigraphy**

127 In the map area, the Dora-Maira consists of a Paleozoic basement and a thin Mesozoic
128 cover.

129 The Paleozoic basement corresponds to a pre-Carboniferous polymetamorphic complex
130 that mainly consists of medium-grained garnet-chloritoid micaschist (Fig. 2a). This
131 micaschist locally preserves Variscan-related medium grade mineral relics,
132 corresponding to garnet porphyroblasts (Fig. 2a) and muscovite lepidoblasts. The
133 garnet-chloritoid micaschist embeds layers and bodies of impure marble, metabasite and
134 gneisses. The impure marble is several metres-thick and is characterized by a mylonitic
135 fabric defined by alternating centimetres-thick grey (calcite-rich) and yellow-whitish
136 (dolomite-rich) layers (Fig. 2b). It also consists of subordinate chlorite, white mica,
137 tremolite and clinopyroxene (diopside), which likely represents a relic of the Variscan
138 mineral assemblage. The metabasite crops out both as boudinage layers (up to ten of
139 meters-thick) and small boudins (decimetre in size), and occurs within the micaschist
140 (Fig. 2c) and marble (Fig. 2b and Fig. 2d). The metabasite, despite of widespread re-
141 equilibration under greenschist-facies conditions, preserves relics of the eclogitic
142 assemblage consisting of garnet, omphacite, white mica (phengite) and rutile. The up to
143 tens of meters-thick gneisses can be distinguished in fine-grained layered gneiss (Fig.
144 2e) and coarse-grained K-feldspar-bearing ones (Fig. 2f and 2g). The former is
145 characterized by a compositional banding defined by alternating centimetres-thick light
146 grey and dark green layers (Fig. 2e), which mainly consist of albite + quartz + garnet +
147 phengite, and epidote + phengite + albite + quartz + Ca-amphibole, respectively. The
148 coarse-grained K-feldspar-bearing (Fig. 2f and 2g) gneiss also consists of quartz, albite,
149 phengite, epidote and biotite, and is characterized by occurrences of centimetres to
150 decimetres-thick levels of silvery micaschist (Fig. 2h), which is made up of quartz and
151 white mica (phengite).

152 The Mesozoic cover consists of massive white marbles and overlying calcschists. The
153 former is made up of calcite, with minor dolomite and white mica (phengite), and is
154 locally characterized by occurrence of few centimetres-thick metapelitic layers. The
155 calcschists are fine- to medium-grained and consist of calcite, quartz, white mica
156 (phengite), with minor chlorite and albite. Similar cover successions occur in other
157 sectors along the western edge of the Dora-Maira and have been interpreted as Middle
158 Triassic to Early Jurassic in age (Balestro et al., 2013, 2015).

159

160 **5. Structures**

161 Variscan-related structures have been recognized exclusively as microscale relics,
162 whereas Alpine structures are widely exposed at mesoscale and result from three main
163 syn-netamorphic deformation phases (named D₁, D₂ and D₃).

164 The D₁ developed during the eclogite-facies metamorphism and is responsible for the
165 development of a mylonitic foliation (i.e. the S₁; Fig. 3a). Symmetric and asymmetric
166 boudins of metabasite occurring within the impure marble, garnet-chloritoid micaschist
167 and layered gneisses, are interpreted to be related to the S₁-parallel stretching during D₁
168 simple shear.

169 The D₂ developed under the early blueschist-facies metamorphic re-equilibration and is
170 defined by isoclinal folds, with thickened hinges and thinned limbs (Fig. 3a and 3b),
171 characterized by N-S sub-horizontal axes and W-dipping axial planes (Fig. 4). The pre-
172 existing S₁ mylonitic fabric is clearly deformed by D₂ folds that developed an axial
173 plane foliation (i.e. the S₂), which corresponds to the W-dipping main regional foliation
174 (Fig. 4). At the map scale, an example of these structures is the folding of the impure
175 marble body in the central part of the map area (see also cross section E-F).

176 D₂ isoclinal folds and their axial plane foliation appear to be gently refolded by D₃ folds
177 (Fig. 3c and 3d), especially in the western part of the map area. D₃ folds developed
178 under greenschist-facies metamorphic condition and are characterized both by tight
179 profiles in the form of crenulation folds (Fig. 3c) and open to gentle geometries. D₃
180 axial planes weakly dip towards the NE and D₃ axes are on average sub-horizontal with
181 a roughly N-S trend (Fig. 4).

182 A last significant phase of deformation is a stage of extensional faulting that post-dates
183 the syn-metamorphic structures and has been also described outside the study area
184 (Perrone et al., 2009, 2011). Extensional faults are nearly NE-SW striking and NW
185 steeply dipping (Fig. 5a), and their displacements range from a minimum of a few
186 centimetres to a maximum of several metres (Fig. 5b, 5c, 5d and 5e). Fault rocks are
187 mostly represented by tectonic breccia that are well exposed close to Fontane locality
188 and in the northern part of the map area (i.e., the “Meison breccias” of Novarese, 1895,
189 Borghi et al., 1984). At map scale, extensional faults are expressed as NE-SW
190 hectometre- to kilometre-scale fault segments arranged in en-echelon, left-stepping
191 geometrical pattern, and spaced several hundreds of metres.

192

193 **6. Geometry of the FTM**

194 Defining the structure and extent of the FTM is of critical importance both for
195 understanding the origin of talc and for any industrial operations related with its
196 extraction. Talc is not distributed in continuous horizons but forms isolated bodies
197 embedded within the garnet-chloritoid micaschist and the K-feldspar-bearing gneiss
198 closely associated with the impure marble.
199 Talc bodies appear to define lenses with a shape similar to that of the boudins of
200 metabasite (see cross section C-D), suggesting that their early geometry resulted from
201 D₁ deformation. These lenses were later deformed during the D₂ phase and now outcrop
202 in the form of thickened hinges of rootless folds, and were slightly affected by the D₃
203 that seems to cause minor changes in the dip of the isolated lenses.
204 Finally, extensional faults that intersect talc bodies at depth appear to be responsible for
205 their dislocations towards the NW with displacements of up to several tens of metres
206 (see cross section A-B).

207

208 **7. Conclusions**

209 The 1:5,000 scale Geological Map of the Fontane Talc Mineralization gives new
210 information for interpreting the origin and distribution of talc bodies.
211 Detailed geological mapping and underground observations highlight that the talc
212 bodies (*i*) are embedded within a pre-Carboniferous polymetamorphic complex, (*ii*)
213 occur along a well-defined lithostratigraphic association between micaschist, marble
214 and gneiss, and (*iii*) never occur within the Mesozoic cover.
215 Structural analysis highlights that the talc bodies were clearly deformed during Alpine-
216 related deformation phases (i.e. the D₁, D₂ and D₃ phases) and, therefore, their genesis
217 predate Alpine tectonics.
218 These considerations may be useful for future research regarding the origin of the FTM
219 as well as other talc mineralizations occurring along the western edge of the Dora-
220 Maira. Pre-rift tectonics (and associated metasomatic processes?) which affected the
221 paleo-European continental margin likely appear as a geodynamic context wherein talc
222 could be formed. Extensional tectonics model is described for other important talc
223 mineralization, such as the Trimouns Talc Deposit in the Pyrenees ([Schärer et al.,](#)
224 [1999](#)).
225 Moreover, the here defined lithostratigraphic and structural characterization of the FTM
226 may represent a useful geological model for new mineral explorations outside the map
227 area.

228

229

230 **Software**

231 The geological map was digitized using the software ArcMap of the suite ArcGis

232 Desktop (v. 9.3) by ESRI®.

233

234 **Acknowledgements**

235 We thank E. Casciello, P. Conti and B. Cattoor for constructive reviews, and R.

236 Orndorff for editorial handling. Giulia Codegone, and Elena Cerino Abdin are

237 acknowledged for their help during fieldwork. This research has been supported by “ex

238 60%–2013 and 2014” Università degli Studi di Torino and by the Italian Ministry of

239 University and Research Cofin-PRIN 2010/2011 (“Subduction and exhumation of

240 continental lithosphere: Implications on orogenic architecture, environment and

241 climate”).

242

243

244 **References**

245

246 Balestro, G., Fioraso, G. and Lombardo, B. (2013). Geological map of the Monviso

247 massif (Western Alps). *Journal of Maps*, 9, 623-634.

248

249 Balestro, G., Lombardo, B., Vaggelli, G., Borghi, A., Festa, A., and Gattiglio, M.

250 (2014). Tectonostratigraphy of the northern Monviso Meta-ophiolite Complex (Western

251 Alps). *Italian Journal of Geosciences*, 133 (3), 409-426.

252

253 Balestro, G., Festa, A., and Tartarotti, P. (2015). Tectonic significance of different

254 block-in-matrix structures in exhumed convergent plate margins: examples from

255 oceanic and continental HP rocks in Inner Western Alps (northwest Italy). *International*

256 *Geology Review*, 57 (5-8), 581-605.

257

258 Bigi, G., Castellarin, A., Coli, M., Dal Piaz, G. V., Sartori, R., Scandone, P. and Vai,

259 G. B. (1990). Structural Model of Italy, sheet 1, C.N.R., *Progetto Finalizzato*

260 *Geodinamica, Litografia SELCA*, Firenze.

261

262 Borghi A. & Sandrone R. (1990). Structural and metamorphic constraints to the
263 evolution of a NW sector of the Dora-Maira Massif (Western Alps). *Memorie della*
264 *Società Geologica Italiana*, 45, 131-141.
265

266 Borghi A., Cadoppi P., Porro A., Sacchi R. & Sandrone R. (1984). Osservazioni
267 geologiche nella Val Germanasca e nella media Val Chisone (Alpi Cozie). *Bollettino*
268 *del Museo Regionale di Scienze Naturali di Torino*, 2, 503-530.
269

270 Bussy F. & Cadoppi P. (1996). U-Pb zircon dating of granitoids from the Dora-Maira
271 massif (Western Italian Alps). *Schweiz. Mineral. Petrogr. Mitt.*, 76, 217-233.
272

273 Cadoppi P. (1990). Geologia del basamento cristallino nel settore settentrionale del
274 Massiccio Dora-Maira (Alpi Occidentali). Ph.D thesis, University of Turin, Turin-Italy:
275 pp. 208.
276

277 Cadoppi P. & Tallone S. (1992). Structural and lithostratigraphic heterogeneity of the
278 northern part of Dora-Maira massif (Western Alps). *Atti Ticinesi di Scienze della Terra*,
279 35, 9-18.
280

281 Cadoppi P., Castelletto M., Sacchi R., Baggio P., Carraro F. & Giraud V. (2002). Note
282 illustrative della Carta Geologica d'Italia alla scala 1:50.000 - Foglio 154, Susa. *Servizio*
283 *Geologico d'Italia*, pp. 127.
284

285 Camanni (2010). Geological-structural analysis and 3D modelling of the Fontane talc
286 mineralization (Germanasca Valley, Inner Cottian Alps). Unpublished MSc thesis,
287 Univ. Turin: pp. 126.
288

289 Chopin C., Henry C. & Michard A. (1991). Geology and petrology of the coesite-
290 bearing terrain, Dora Maira massif, Western Alps. *European Journal Mineral.*, 3, 263-
291 291.
292

293 Dal Piaz, G.V., Bistacchi, A., Massironi, M. (2003). Geological outline of the Alps.
294 *Episodes*, 26, 175–180.
295

296 Damiano A. (1997). Studio geologico delle mineralizzazioni a talco nelle valli
297 Germanasca, Chisone e Pellice (Massiccio Dora-Maira, Alpi Cozie). Unpublished
298 degree thesis, Univ. Turin: pp. 145.
299
300 Grill E., Pagliani G. & Sacchi L. (1955). La genesi del talco della valle della
301 Germanasca (Alpi Cozie). *Ist. Lombardo Sc. e Lett.*, 88, 442-490.
302
303 Mattiolo, E., Novarese, V., Franchi, S. and Stella, A. (1913). Carta Geologica d'Italia a
304 scala 1:100.000, foglio 67 Pinerolo, *Litografia Artistica Cartografica, Roma*.
305
306 Novarese V. (1895). Sul rilevamento geologico eseguito nel 1894 in valle della
307 Germanasca (Alpi Cozie). *Boll. R. Comit. Geol. It.*, 26: 253-282.
308
309 Peretti L. (1966). Geologia e genesi dei giacimenti di talco nel Pinerolese. *Boll. Ass.*
310 *Min. Sub.*, 3: 283-306.
311
312 Perrone G., Cadoppi P., Tallone S. & Balestro G. (2011). Post-collisional tectonics in
313 the Northern Cottian Alps (Italian Western Alps). *Int. J. Earth. Sci. (Geol Rundsch)*,
314 100, 1349–1373, DOI 10.1007/s00531-010-0534-1
315
316 Perrone G., Morelli M., Cadoppi P., Tallone S. & Giardino M. (2009). A
317 multidisciplinary approach to the study of the fault network in the internal Cottian Alps
318 (Western Alps). *Ital. J. Geosci.*, 128, 541-549.
319
320 Ramsay, J.G. (1967). Folding and fracturing of rocks. New York, McGraw-Hill Book
321 Company, pp. 560.
322
323 Sandrone R. & Zucchetti S. (1989). Geology of the Italian high-quality cosmetic talc
324 from the Pinerolo district (Western Alps). Proceedings of Symposium “Zuffardi’
325 days”, Cagliari, 1988.
326
327 Sandrone R., Borghi A., Carosso G., Morsetti C., Tagliano C. & Zucchetti S. (1990).
328 Geometry of the talc deposit of Fontane, and structural evolution of the area (Dora
329 Maira Massif, Western Alps). *Boll. Assoc. Min. Subalpina*, 27: 45-62.

330

331 Sandrone R., Cadoppi P., Sacchi R. & Vialon P. (1993). The Dora-Maira Massif. In:
332 von Raumer J.F. & Neubauer F. (eds.), “Pre-Mesozoic Geology in the Alps”, *Springer-*
333 *Verlag, Berlin Heidelberg New York*: 317-325.

334

335 Sandrone R., Trogolo Got D., Respino D & Zucchetti S. (1987). Osservazioni geo-
336 giacimentologiche sulla miniera di talco di Fontane (Val Germanasca, Alpi Cozie).
337 *Mem. Sci. Geol. Padova*, 39: 175-186.

338

339 Schärer U., de Parseval Ph., Polvé M., de Saint Blanquat M. (1999). Formation of the
340 Trimouns talc-chlorite deposit (Pyrenees) from persistent hydrothermal activity between
341 112 and 97 Ma. *Terra Nova*, 11: 30-37.

342

343 Tricart, P., and Schwartz, S. (2006). A north-south section across the Queyras Schistes
344 lustrés (Piedmont zone, western Alps): Syn-collision refolding of a subduction wedge:
345 *Eclogae Geologicae Helvetiae*, 99, p. 429–442

346

347 Vialon P. (1966). Etude géologique du Massif Cristallin Dora-Maira (Alpes Cottiennes
348 internes-Italie). *Trav. Lab. Géol. Grenoble*, 4: pp. 293.

349

350 Zucchetti S. (1969) Osservazioni sui giacimenti di talco della Val Germanasca (Torino)
351 - Nota Preliminare. *Boll. Ass. Min. Sub.*, 6: 240-248.

352

353 Zucchetti S. (1972). Caratteri lito-mineralogici e genetici dei giacimenti di talco della
354 Val Germanasca nelle Alpi Occidentali (Italia). Proceedings of the 2. International
355 Symposium on the Mineral Deposits of the Alps, Ljubljana, S. Kolenko: 263-279

356

357 Wheeler, J. (1991). Structural evolution of a subducted continental sliver: The northern
358 Dora Maira massif, Italian Alps: *Journal of the Geological Society of London*, 148:.
359 1101–1113.

360

361

362

363 **Figure captions**

364

365 Figure 1: Localization of the Fontane Talc Mineralization in the tectonic map of the
366 Western Alps.

367

368 Figure 2: a) medium-grained garnet-chloritoid micaschist with porphyroblasts of
369 centimetric pre-Alpine garnet (road to Rodoretto Village); b) impure marble with
370 mylonitic fabric defined by a compositional banding of grey (calcite-rich) and yellow-
371 whitish (dolomite-rich) alternating layers. Black arrows indicate a boudinated
372 centimetres-thick layer of metabasite occurring within the marble (Rocca Bianca quarry,
373 just outside the study area); c) and d) boudins of metabasite embedded into the
374 micaschist and marble, respectively (road to Rodoretto Village and Gianna mine
375 tunnel); e) layered gneiss with its characteristic compositional banding (near the bridge
376 on the mouth of the Rodoretto Stream in the Germanasca Stream); f) outcrop view and
377 g) detail of the K-feldspar-bearing gneiss (road to Rodoretto Village); h) decimetres-
378 thick level of silvery micaschist embedded in the K-feldspar-bearing gneiss
379 (Serrevecchio locality).

380

381 Figure 3: D2 and D3 structures. a) S_1 mylonitic layering of impure marble fabric
382 deformed by D_2 folds (Maiera quarry, near the study area); b) isoclinal D_2 folds with
383 thickened hinges occurring within the garnet-chloritoid micaschist (road to Rodoretto
384 Village); c) D_3 structures folding of S_2 foliation within the garnet-chloritoid micaschists
385 (road to Rodoretto Village); d) Type-3 interference pattern (Ramsay, 1967) between D_2
386 and D_3 folds and related axial plane foliation (S_2 and S_3), occurring within the impure
387 marble (ma) and garnet-chloritoid micaschist (ms) (S_M corresponds to the S_1 foliation;
388 sample from the Gianna mine tunnel).

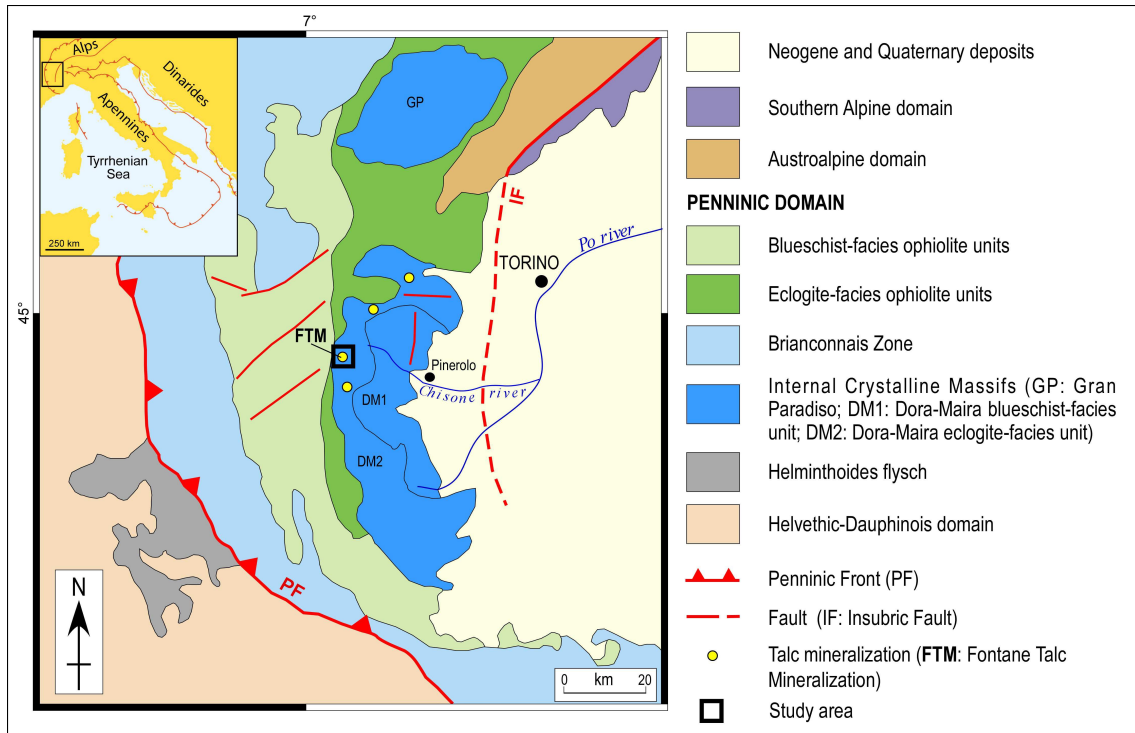
389

390 Figure 4: contoured stereographic projections (equal-area, lower hemisphere) of the D_2
391 and D_3 structures. The great circles show the mean orientation. N is the number of data.

392

393 Figure 5: a) contoured stereographic projections (equal-area, lower hemisphere
394 projections) of the extensional faults. The great circles show the mean fault

395 plane orientations. Data contoured at $n = 2, 4, 6, 8, 10, 12$ times uniform. N is the
396 number of data. The red, blue and green squares represent the maximum (P),
397 intermediate and minimum (T) shortening axes for the average incremental strain
398 solution, respectively; b) and c) Riedel shear-sense indicators (R and R') and inflection
399 of the S_2 foliation (dashed white line) along normal fault planes occurring within the
400 garnet-chloritoid micaschist (entrance of the Gianna mine tunnel); d) Plurimetric
401 displacement of the contact (dashed white line) between the garnet-chloritoid
402 micaschist (above) and impure marbles (below) (E of Fontane Village); e)
403 pluridecimetric displacement of the contact (dashed white line) between the K-feldspar-
404 bearing gneiss (above) and garnet-chloritoid micaschist (below) (Gianna mine tunnel).
405

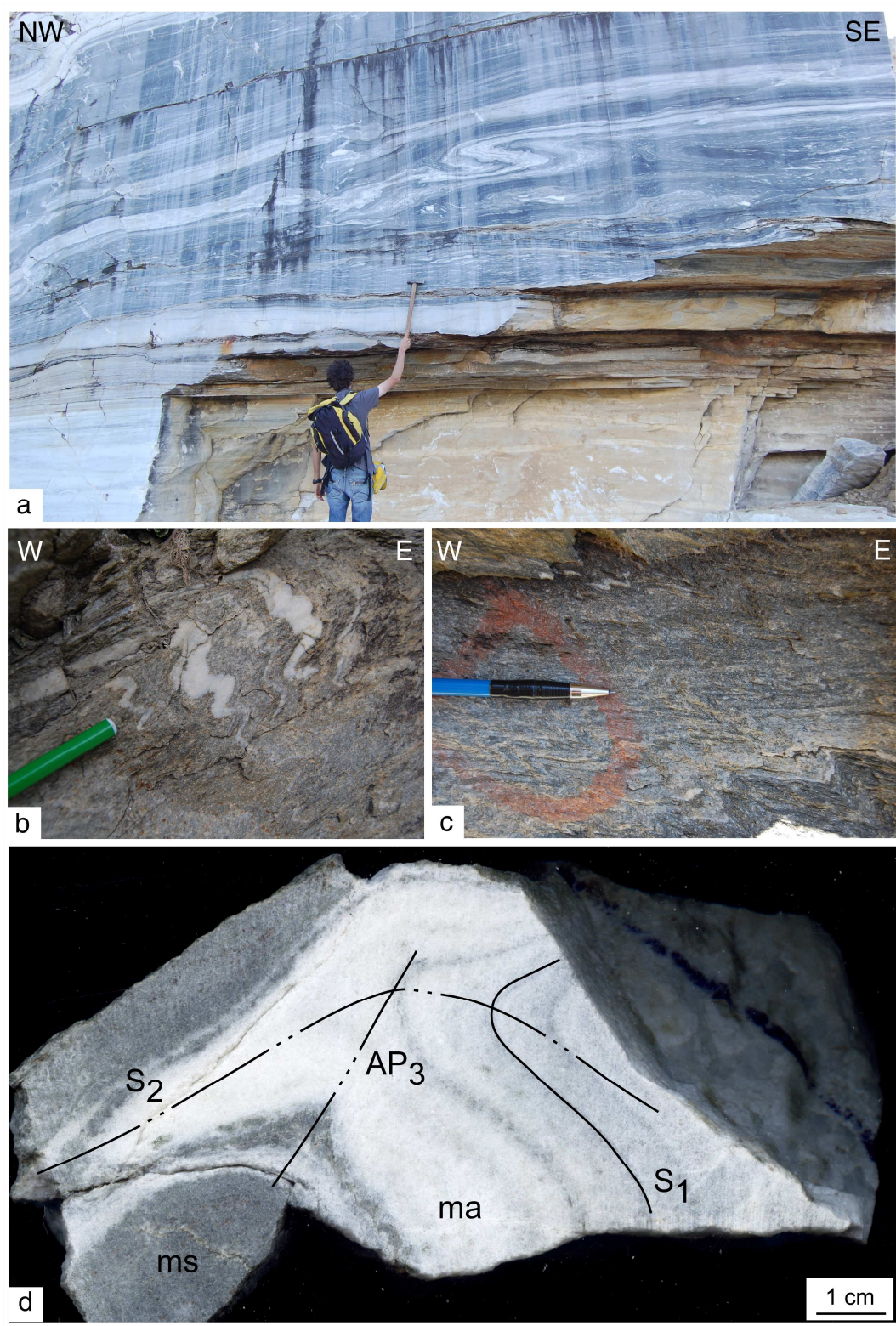


406

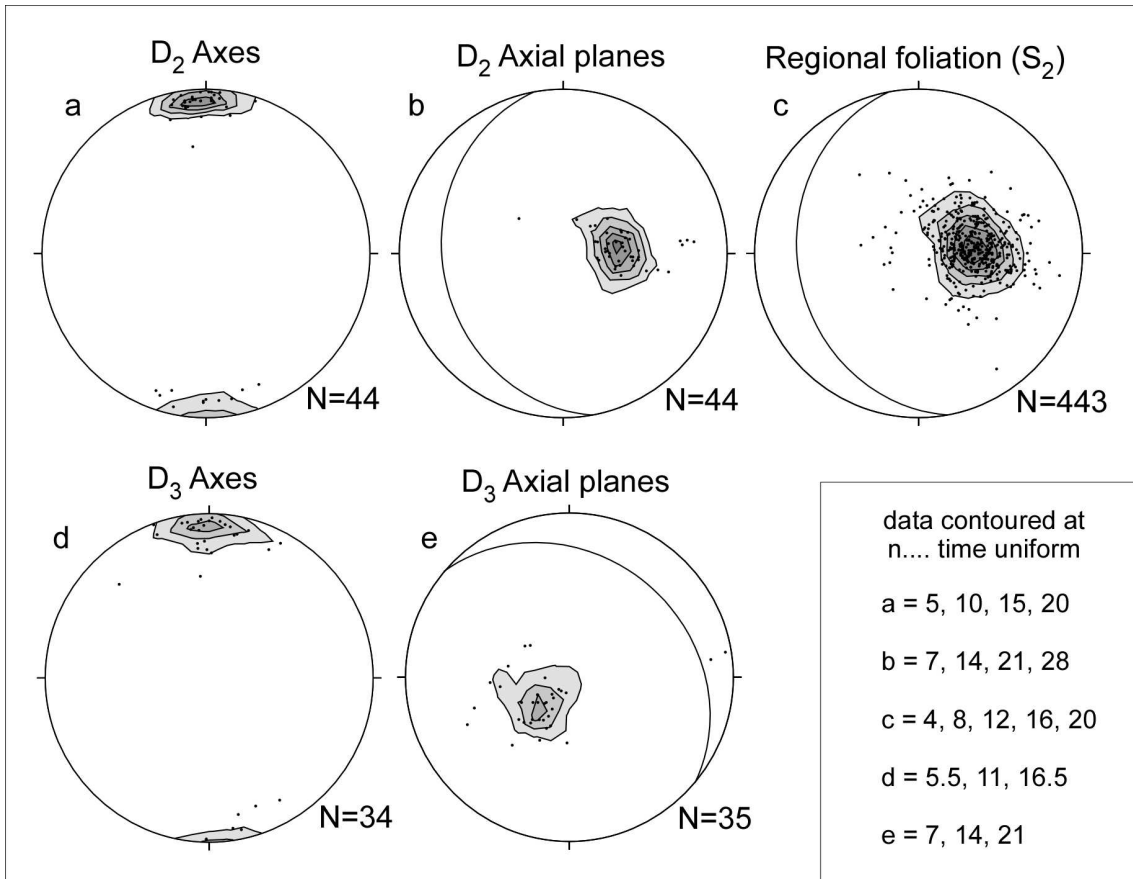
407



408
409

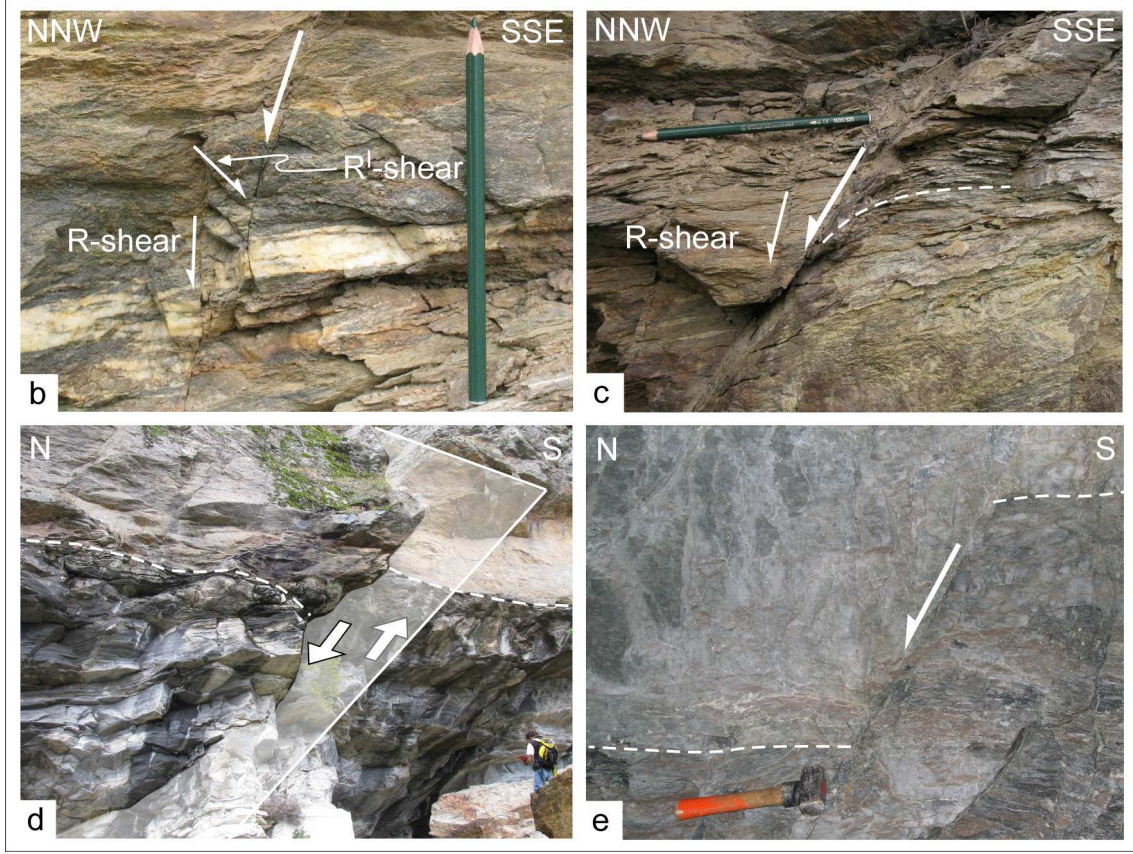
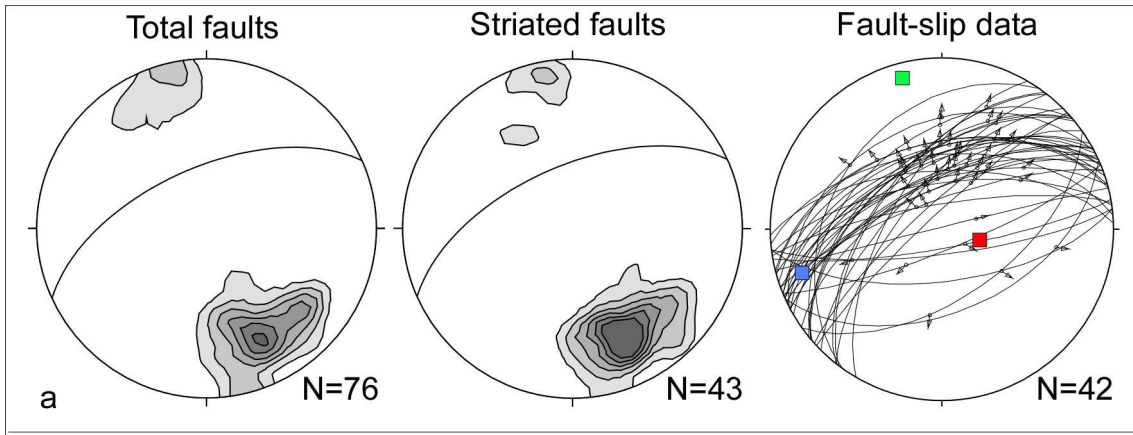


410
 411



412

413



414
415